Structural analysis of the natural clinker-based analcime (NC-ANA) by X-ray powder diffraction and solid-state ^{29}Si and ^{27}al nuclear magnetic resonance spectroscopy

Análisis estructural de la analcima obtenida a partir de clinker natural (NC-ANA) mediante difracción de rayos X de muestras policristalinas y espectroscopia de resonancia magnética nuclear de estado sólido de ^{29}Si y ^{27}Al

Mario Alberto Macías López[1], José Antonio Henao Martínez[1], Carlos Alberto Ríos Reyes[2]*

[1]Grupo de Investigación en Química Estructural (GIQUE). Escuela de Química. Universidad Industrial de Santander. A.A 678. Bucaramanga. Colombia.

[2]Grupo de Investigación en Mineralogía, Petrología y Geoquímica (MINPETGEO). Escuela de Geología. Universidad Industrial de Santander. A.A 678. Bucaramanga. Colombia.

(Recibido el 8 de septiembre de 2010. Aceptado el 10 de noviembre de 2011)

Abstract

The natural clinker-based analcime (NC-ANA) framework was synthesized by the conventional hydrothermal alkaline activation method. The synthesized zeotype was characterized by X-ray powder diffraction (XRPD) analysis and solid-state ^{29}Si and ^{27}Al nuclear magnetic resonance (NMR) spectroscopy. XRPD data indicate that the NC-ANA zeotype framework crystallized in the rhombohedral space group *R*-3, with unit cell parameters a = 11,8995(6) Å, α = 109,472(2)°, V = 1.300,69(1) Å^3, Z = 8. ^{29}Si NMR data reveal a number of resonance lines, with a full width at half height typically less than 2 ppm. The attribution of NMR lines to Qn groups was done by considering the stoichiometry and crystallographic data of the NC-ANA.

----- *Keywords:* analcime, framework, natural clinker, Rieltveld method, NMR spectroscopy

* Autor de correspondencia: telefax: 57 + 7 + 634 34 57, correo electrónico: carios@uis.edu.co (C. Ríos)

Resumen

La estructura de la analcima a partir de clinker natural (NC-ANA) fue sintetizada a partir del método de tratamiento hidrotérmico convencional de activación alcalina. El zeotipo sintetizado se caracterizó mediante difracción de rayos-X de muestras en polvo (DRXP) y espectroscopia de resonancia magnética nuclear (RMN) de estado sólido de ^{29}Si y ^{27}Al. Los datos estructurales obtenidos a partir del refinamiento de los datos de DRX indican que la estructura del zeotipo NC-ANA cristaliza en el grupo espacial romboédrico *R*-3, con parámetros de celda unidad a = 11,8995(6) Å, α = 109,472(2)°, V = 1.300,69(1): Å^3, Z = 8. Los datos de RMN de ^{29}Si revelan la ocurrencia de una serie de líneas de resonancia, con un ancho del pico a mitad de la altura máxima típicamente inferior a 2 ppm. La asignación de las líneas de RMN para los grupos Qn se realizó teniendo en cuenta los datos estequiométricos y cristalográficos de la NC-ANA.

----- *Palabras clave:* analcima, estructura, clinker natural, método de Rieltveld, espectroscopia de RMN

Introduction

Analcime belongs to minerals of tectosilicate group with zeolitic structure [1]. Due to the similarity of structure, under natural conditions it often crystallizes in magmatic vein rocks with a low SiO_2 content, as well as in metamorphic and hydrothermal vein rocks in paragenetic associations together with other zeolites [2]. The crystal structure of analcime $NaAlSi_2O_6 \cdot H_2O$ was determined by Taylor [3] but several other studies have been made [4-6] in view of the apparent incompatibility with cubic symmetry (space group *Ia*3*d*) of certain properties both physical (especially the weak but definite optical birefringence of some samples) and chemical (particularly the remarkable constancy of the Al/Si ratio among naturally occurring analcimes). It is well known for a long time that many analcimes exhibit some deviation from cubic symmetry [7-9] and little was known about the real symmetry of non-cubic analcime. Mazzi et al. [10] showed the symmetry of non-cubic leucite to be tetragonal $I4_1/a$ and considered it a possible symmetry also for non-cubic analcime. Yokomori and Idaka [11] studied diffraction data with both cubic and trigonal system from the same crystal of analcime and demonstrated that every pseudo-cubic or average cubic analcime is really trigonal with the unit cell size a half of the cubic cell size. Harada and Sudo [8] suggested a monoclinic symmetry as probable for analcime, because the extrapolation of β values in the wairakite-analcime series gives β = 90.12° for pure analcime. Pechar [12] performed an X-ray and neutron diffraction analysis on a single crystal of natural monoclinic analcime, which is topologically the same as in the cubic modification. Mazzi and Galli [9] refined the crystal structure of analcime and reported the symmetry for non-cubic analcimes to be tetragonal ($I4_2/acd$) and orthorhombic (*Ibca*). They suggested that this difference of symmetries was caused by ordering of Al and Si. Akizuki [13] studied thin section of analcime and found optical anomaly and suggested that this optical anomaly was caused by ordering of Al and Si during crystal growth. The purpose of this work was characterized structurally the natural clinker-based analcime (NC-ANA) framework by the aid of XRPD analysis using the Rietveld method and solid-state ^{29}Si and ^{27}Al NMR spectroscopy.

Materials and methods

Natural clinker-based analcime

The zeotype ANA framework of interest in this study corresponds to the NC-ANA prepared in

a previous work by Sandoval et al. [14] after hydrothermal treatment of natural clinker under the following experimental conditions: NaOH solution 3M; alkaline solution/natural clinker ratio = 8ml/g; hydrothermal temperature = 150 ºC and reaction time = 24h.

X-ray powder diffraction analyses

The XRPD pattern of NC-ANA was recorded with a D8FOCUS BRUKER diffractometer operating in Bragg-Brentano geometry equipped with an X-ray tube (Cu-Kα radiation: λ = 1.5406 Å, 40 kV and 40 mA) using a nickel filter and a 1-dimensional LynxEye detector. A fixed antiscatter slit of 8 mm, receiving slit (RS) of 1 mm, soller slits of (SS) of 2.5º and a detector slit of 3 mm were used. Data collection was carried out in the 2θ range of 2-70°, with a step size of 0.02° (2θ) and counting time of 1 s/ step. The XRPD reflexions for NC-ANA were indexed with the computer program DICVOL04 [15] using an absolute error of 0.03º (2θ) in the calculations, and the initial lattice parameter values for Rietveld refinement were estimated. Initial atomic coordinates and isotropic temperature factors were taken from the model reported by Yokomori and Idaka [11]. The XRPD pattern was refined by the whole pattern fitting MAUD (Materials Analysis Using Diffraction) program based on Rietveld method [16-17] using a pseudo-Voigt peak-shape profile [18-19] and adopting an iterative least-square procedure through minimization of the residual parameters R_w, R_B and R_{exp} [20].

Solid-state ^{29}Si and ^{27}Al nuclear magnetic resonance spectroscopy

Solid-state ^{29}Si and ^{27}Al NMR spectra of NC-ANA were recorded at room temperature on a Varian VNMRS spectrometer under the following analytical conditions for ^{29}Si and ^{27}Al, respectively: MAS probe 7.5 and 4.0 mm; frequency 59.56 and 104.20 MHz; spectral width 30.0 and 417.7 kHz; acquisition time 40 and 20 μs; recycle time 120 and 0.2 sec; number of repetitions 42-468 and 12.200-28.000 Hz; spinning rate 5.010-5.050 and 14.000 Hz; pulse angle (DP) 90.0 and 18.9º. Spectral referencing is with respect to tetramethylsilane (TMS) for ^{29}Si and 1 M $AlCl_3$ aqueous solution for ^{27}Al.

Results and discussion

Rietveld refinement of the XRPD pattern

Figure 1 shows the observed, calculated and difference profiles for the XRPD data of NC-ANA. The main crystalline phase identified corresponds to the ANA-type structure, although few extra lines reveal the occurrence of traces of anatase and ilmenite. The corresponding difference between the observed and calculated profiles shows good fit for the refined parameters. We have observed in the refined XRPD pattern a preferential orientation effect on the (011) reflection, similar to X-ray analysis of analcime zeolite fibers prepared conveniently and efficiently by the in situ TPAOH template electrostatic self-assembly technique as reported by Liu et al [21].

The Rietveld refinement details obtained for NC-ANA are presented in table 1. The refinement of the XRPD data reveals that the as-synthesized ANA-type structure crystallizes in the rhombohedral space group *R*-3 (No. 148) and yielded the lattice parameters a = 11.8995(6) Å, α = 109.472(2)°, V = 1300.69(1) Å^3, Z = 8. These results are in excellent agreement with those determined by Yokomori and Idaka [11]. The ANA-type structure was refined in all pseudo-cubic structures (tetragonal, orthorhombic and rhombohedral). However, the best R-factors were obtained for the rhombohedral structure. The final agreement values for the refinement are R_W = 10.92%, R_B = 8.39%, R_{exp} = 6.95%, and χ^2 = 1.57%. The refined weight fraction value of this structure was 98.4(2)%.

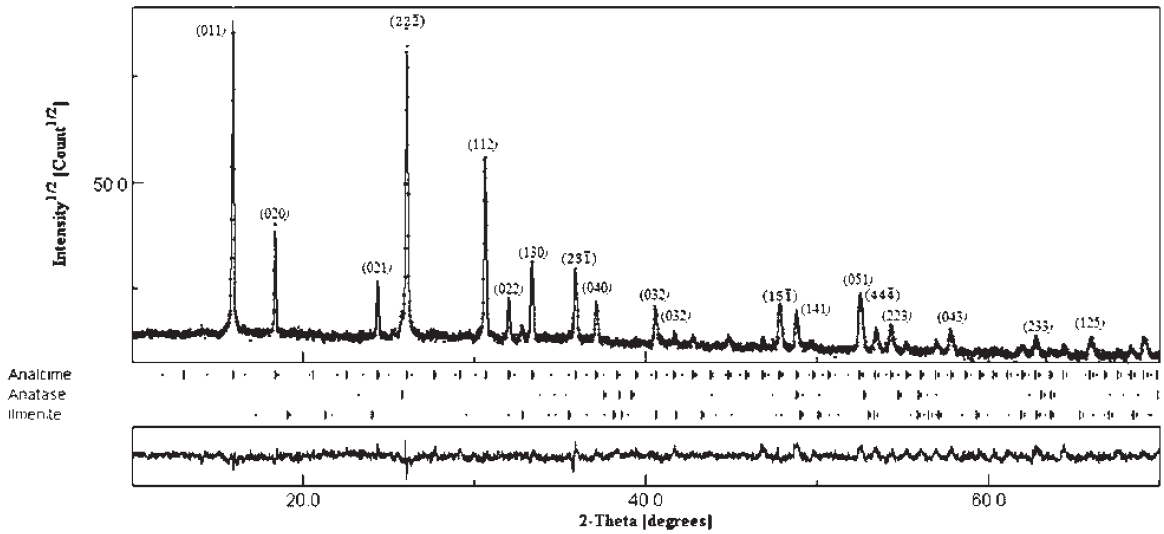

Figure 1 Observed (cross-hatches) and calculated (continuous lines) profiles and the corresponding difference diagram of NC-ANA (λ = 1.5406 Å)

Table 1 The Rietveld refinement details obtained for NC-ANA

Molecular fórmula	$Na_{0.931}(Al_1SiO_6)H_2O$
Molecular weight (g/mol)	218,55
a (Å)	11,8995(6)
α (°)	109,472(2)
V (Å^3)	1.300,69(1)
Z	8
Space group	R-3 (N° 148)
D_x (g/cm^3)	2,22
Rw	10,9
R_B	8,38
Rexp	6,95
χ^2	1,57
Weight fraction (%)	98,4(2)

The final atomic coordinates and isotropic displacement parameters with standard uncertainties in parentheses are shown in table 2. The tetrahedral occupancy of Si and Al was constrained to have the same atomic coordinates and isotropic displacement parameters with occupation factors of 0.6497 and 0.3503 for Si and Al, respectively, which were calculated from X-ray fluorescence spectroscopy data reported by Sandoval et al. [14]. These values are different from those reported by Yokomori and Idaka [11]. Relatively high values of isotropic displacement parameters, 6.73(6) and 6.80(2) for Ow_1 and Ow_2 atoms, respectively, reveal the liberated motion of the H_2O molecules. On the other hand, the rest of the oxygen atoms show lower values due to the tetrahedral coordination.

The selected bond distances (Å) and angles (deg.) for NC-ANA are listed in tables 3 and 4, respectively. Figure 2 shows the NC-ANA structure projected down the rotation axis. The ANA-type structure exhibits a disordered distribution of Si and Al atoms in tetrahedral sites. The Si-Al distribution produces a distortion of lattice parameters and angles of the structure compared with the cubic, orthorhombic and tetragonal considerations. The final framework distances are all within the ranges expected for Si-O, Al-O and Na-O bonds. However, the O-Si-O and O-Al-O angles are not close to the ideal tetrahedral angle. The cation positions for Na are represented by two sites. In the site 1, Na is coordinated to the oxygen atoms Ow1 with bond distance of 1.99(4). Each Na cation is

surrounded by four oxygen atoms (O1, O2, O6, O7) and two H_2O molecules (Owl, Ow2). In the site 2, Na is coordinated to the oxygen atoms Ow2 (located on the center of the channels) with bond distance of 2.33(2) and 2.44(5). Each Na cation is also surrounded by the oxygen atoms (O3, O5, O8) and two H_2O molecules (Ow2, Ow2a). All Na cations occupy the general position (6f) with occupancy factors for Na1 and Na2 of 0.635 and 0.606, respectively. Consequently, the total number of Na ions is 7.45.

Table 2 Atomic coordinates and equivalent isotropic displacement parameters with standard uncertainties in parentheses for NC-ANA

Atom	*Ox.*	*Site.*	*x*	*y*	*z*	*Foc*	*H*	*Biso (Å2)**
Si1	4+	6f	0.692(3)	0.445(2)	0.455(5)	0.650	0	1.12(2)
Al1	3+	6f	0.692(3)	0.445(2)	0.455(5)	0.350	0	1.12(2)
Si2	4+	6f	0.758(2)	0.305(8)	0.199(2)	0.650	0	1.12(2)
Al2	3+	6f	0.758(2)	0.305(8)	0.199(2)	0.350	0	1.12(2)
Si3	4+	6f	0.784(2)	0.034(6)	0.066(7)	0.650	0	1.12(2)
Al3	3+	6f	0.784(2)	0.034(6)	0.066(7)	0.350	0	1.12(2)
Si4	4+	6f	0.526(8)	0.762(2)	0.968(8)	0.650	0	1.11(2)
Al4	3+	6f	0.526(8)	0.762(2)	0.968(8)	0.350	0	1.11(2)
O1	2-	6f	0.656(6)	0.522(2)	0.407(4)	1	0	2.52(6)
O2	2-	6f	0.884(3)	0.519(3)	0.649(4)	1	0	2.47(6)
O3	2-	6f	0.743(2)	0.375(3)	0.415(2)	1	0	2.42(6)
O4	2-	6f	0.761(2)	0.162(2)	0.168(2)	1	0	2.54(6)
O5	2-	6f	0.594(3)	0.273(2)	0.068(3)	1	0	2.39(6)
O6	2-	6f	0.640(3)	0.874(2)	-0.030(3)	1	0	2.46(6)
O7	2-	6f	0.910(4)	0.008(2)	0.146(4)	1	0	2.48(6)
O8	2-	6f	0.569(3)	0.766(2)	0.100(3)	1	0	2.56(7)
Ow1	2-	2c	0.7437(1)	0.7437(1)	0.7437(1)	1	H2	6.73(6)
Ow2	2-	6f	0.479(4)	-0.0003(5)	0.751(4)	1	H2	6.80(2)
Na1	1+	6f	0.666(2)	0.869(2)	0.750(3)	0.635	0	2.99(7)
Na2	1+	6f	0.579(2)	0.249(3)	0.874(2)	0.606	0	2.85(6)

Site: symmetry multiplicity and Wyckoff symbol; Foc: occupancy factor; H: attached hydrogens; Biso: isotropic displacement parameters.
*Data taken from Yokomori and Idaka [11]

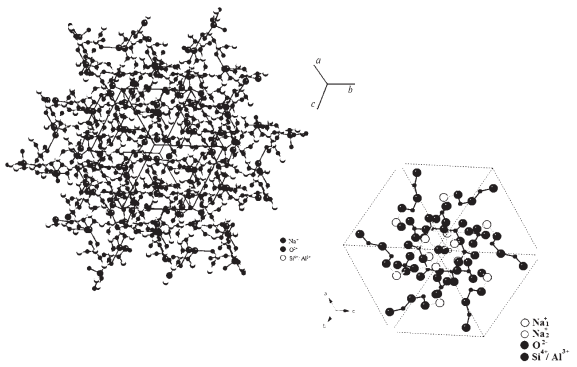

Figure 2 The structure of the NC-ANA projected down the rotation axis

Solid-state ^{29}Si and ^{27}Al NMR spectroscopy

The results of the ^{29}Si and ^{27}Al NMR spectroscopy are in accordance with a model of alternating Si and Al tetrahedra. The ^{29}Si NMR spectrum of the as-synthetized NC-ANA (figure 3) show three peaks at -101.1, -96.2 and -91.1 ppm, corresponding to $Q^4(1Al)$, $Q^4(2Al)$ and $Q^4(3Al)$, respectively, which are characteristic in the ANA-type structure. Relatively intense spinning side bands were noted (not shown). These, with the relatively broad centre band signals, can be accounted for by the known iron content in analcime, which is explained by the occurrence of traces of ilmenite. As a general trend, ^{29}Si chemical shift values became more negative as silicate condensation increases. The ^{27}Al MAS-NMR spectrum in figure 3 is dominated by an intense signal at 58.1 ppm which arises from aluminium in a tetrahedral environment. The studied structure reveals that ^{29}Si occurs in a variety of environments with different crystallographic Si sites and that ^{27}Al is predominantly tetrahedral. According to Sandoval et al. [14], the amount of Al(6) is greatest in the raw natural clinker used as starting material for the synthesis of the ANA-type structure where the initial Al concentration was larger compared with that in the as-synthesized product (NC-ANA). They concluded that the decrease in the Al(6)/Al(4) ratio can be explained by the dissolution of natural clinker, with Al coordination changing from octahedral to tetrahedral, which is consistent with the formation of the zeotype ANA framework.

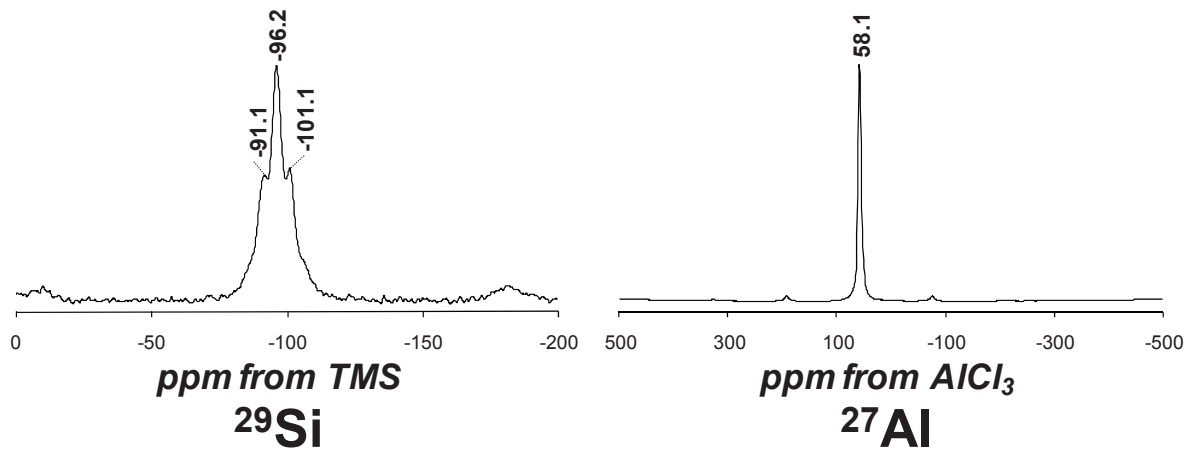

Figure 3 ^{29}Si and ^{27}Al NMR spectra of NC-ANA

Table 5 shows the results for the assignments, chemical shifts, line-widths and intensities of each Q^n group in the deconvoluted ^{29}Si NMR spectrum of NC-ANA. It is known that for each crystallographic site, there are five peaks corresponding to the local Si environments $Q^4(4Al)$ to $Q^4(0Al)$. A number of resonance lines can be observed, with a full width at half

height (FWHH) typically less than 2 ppm. The attribution of NMR lines to Q^n groups was done by considering the stoichiometry and crystallographic data of the ANA-type structure, which represents the main phase in the synthesis product. The Si/Al ratio of this structure was calculated on basis of ^{29}Si NMR data according to the Eq. (1) of Engelhardt and Michel [22].

$$Si/Al = \sum_n I_n / (I_4 + 0.75\, I_3 + 0.5\, I_2 + 0.25 I_1)$$

(I_n = intensity of Q^4/nAl signals in the ^{29}Si NMR spectrum, n = 0–4 without consideration of the signals of the non-zeolitic admixtures); I_1, I_2, I_3 and I_4 represent the intensities of Q^4(1Al), Q^4(2Al), Q^4(3Al) and Q^4(4Al). Figure 4 shows the ^{29}Si NMR spectrum of NC-ANA; five Gaussian deconvolutions were performed because of the presence of Q^4 groups. A percentage of silica with different types Q^n calculated from Gaussian curve fitting shows that the ANA-type structure contains Q^4(0Al), Q^4(1Al), Q^4(2Al), Q^4(3Al) and Q^4(4Al) sites in the ratio 12.4%, 18.1%, 39.3%, 17.9% and 12.3%, respectively, which indicates that the highest intensity peak corresponds to Q^4(2Al) sites. Kirkpatrick [23] have measured the ^{29}Si NMR spectrum for this structure with a Si/Al ratio of 2.0.

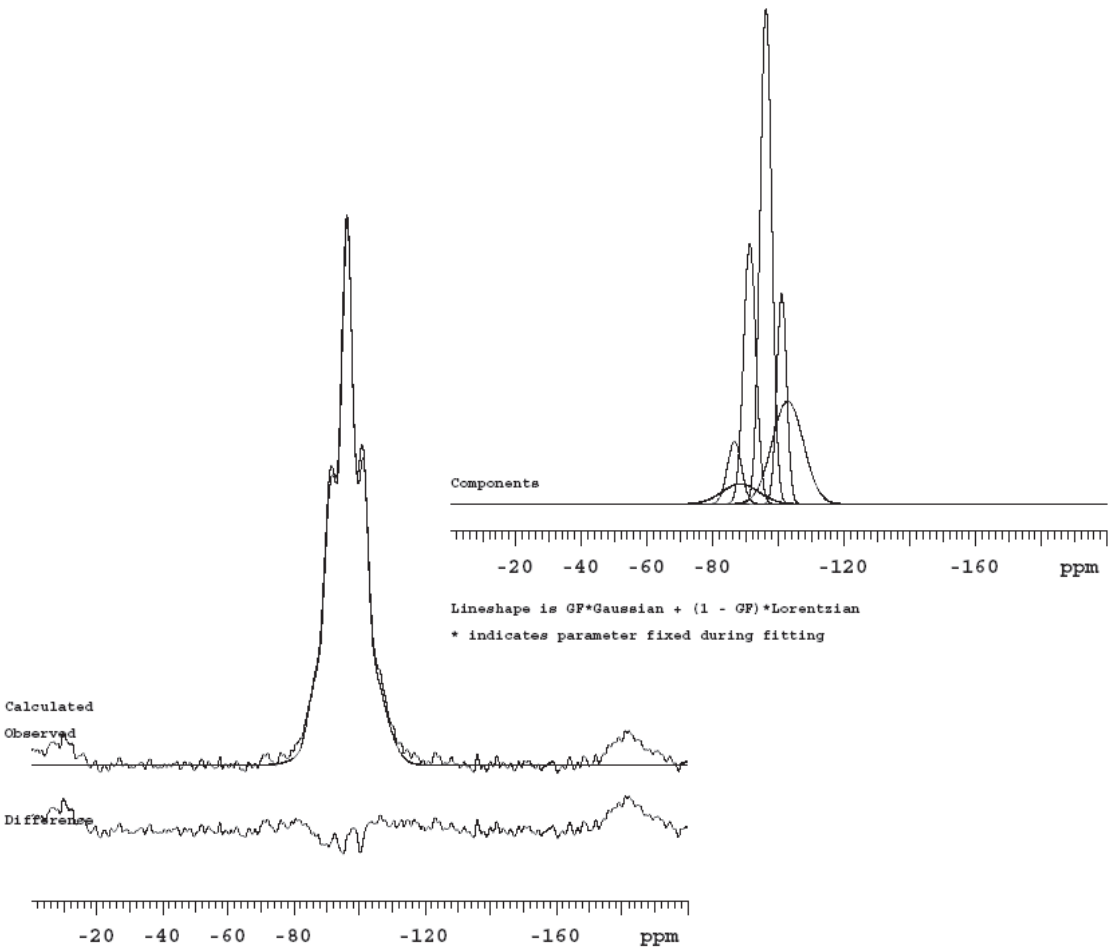

Figure 4 Spectral deconvolution of the ^{29}Si NMR spectrum from NC-ANA. The simulated spectrum is composed of five component lines with Gaussian lineshape. The Difference is the difference between the observed and simulated spectrum

Table 3 Selected bond distances (Å) for NC-ANA

Atom 1	*Atom 2*	*Distance (Å)*	*Atom 1*	*Atom 2*	*Distance (Å)*
Si1	O1	1,34(8)	Si4	O6	1,54(9)
Si1	O1a	1,55(7)	Si4	O8	1,5(1)
Si1	O2	2,26(5)	O1	Na1	2,81(3)
Si1	O3	1,25(6)	O2	Na1	2,76(5)
Si2	O4	1,6(1)	O6	Na1	2,72(5)
Si2	O5	1,86(5)	O7	Na1	2,64(3)
Si2	O8	1,64(6)	Ow1	Na1	1,99(4)
Si3	O4	1,77(7)	O3	Na2	3,02(4)
Si3	O6	1,71(5)	O5	Na2	2,17(5)
Si3	O7	1,56(9)	O8	Na2	1,85(5)
Si4	O2	1,34(7)	Ow2	Na2	2,33(2)
Si4	O5	1,2(1)	Ow2a	Na2	2,44(5)

Table 4 Selected angles (deg.) for NC-ANA

Atom1	*Atom2*	*Atom3*	*Angle(deg.)*	*Atom1*	*Atom2*	*Atom3*	*Angle(deg.)*
O1	Si1	O2	127(3)	O3	Na2	O8	122(2)
O1	Si1	O3	128(4)	O3	Na2	Ow2	90(1)
O1	Si1	O1	121(4)	O3	Na2	O5	172(2)
O2	Si1	O3	76(2)	O3	Na2	Ow2	86(1)
O2	Si1	O1	95(3)	O8	Na2	Ow2	92(2)
O3	Si1	O1	98(3)	O8	Na2	O5	61(2)
O4	Si2	O5	111(3)	O8	Na2	Ow2	109(2)
O4	Si2	O8	114(3)	Ow2	Na2	O5	98(2)
O5	Si2	O8	116(3)	Ow2	Na2	Ow2	157(2)
O4	Si3	O6	113(4)	O5	Na2	Ow2	86(2)
O4	Si3	O7	118(4)	O1	Na1	O2	71(1)
O4	Si3	O7	109(4)	O1	Na1	O6	104(1)
O6	Si3	O7	104(4)	O1	Na1	O7	160(2)
O6	Si3	O7	118(4)	O1	Na1	Ow1	95(1)
O7	Si3	O7	94(4)	O2	Na1	O6	167(2)
O2	Si4	O5	103(6)	O2	Na1	O7	118(2)
O2	Si4	O8	105(5)	O2	Na1	Ow1	100(1)
O2	Si4	O6	101(5)	O6	Na1	O7	63(1)
O5	Si4	O8	99(5)	O6	Na1	Ow1	92(1)
O5	Si4	O6	133(6)	O7	Na1	Ow1	100(1)
O8	Si4	O6	113(5)				

Table 5 Assignments, chemical shifts, line-widths and intensities of the 29Si NMR line to different Q^n units in NC-ANA

Si environment	*Chemical shift[1] (PPM)*	*FWHH[2] (Hz)*	*Intentisity[3] (%)*
Q^4 (4Al)	-87,6	455	12,3
Q^4 (3Al)	-91,6	235	17,9
Q^4 (2Al)	-96,3	243,2	39,3
Q^4 (1Al)	-101,1	221,4	18,1
Q^4 (0Al)	-105,4	501,3	12,4

[1]Relative to tetramethylsilane; [2]Full width at half height; [3]Integrated intensity based on a Gaussian lineshape. Estimated errors: Chemical shift ± 0.5 ppm; FWHH ± 50 Hz; Intensity ± 3.

Conclusions

In the present work, the structural information on zeotype NC-ANA framework synthesized by conventional hydrothermal alkaline activation of natural clinker was obtained from XRPD analysis. The obtained crystallographic data were determined by Rietveld analysis. NC-ANA crystallizes in the rhombohedral space group *R*-3. The unit cell parameters are a = 11.8995(6) Å, α = 109.472(2)°, V = 1.300.69(1) Å^3, Z = 8. The distortion of lattice parameters and angles of the NC-ANA-type structure is attributed to the Si-Al distribution. Solid-state ^{29}Si and ^{27}Al NMR spectroscopy indicates that the as-synthesized NC-ANA exhibited a disordered distribution of Si and Al atoms in tetrahedral sites. In general, the refined data are consistent with experimental and theoretical ones reported in the literature.

Results from this research justify the development of future investigations in the field of the synthesis of new materials that can show a variety of application possibilities in technology. The as-synthesized NC-ANA may be important for technological innovations in selective adsorption and heterogeneous catalysis.

Acknowledgments

We acknowledge the support of the Universidad Industrial de Santander (Colombia) and the University of Durham (England) for providing the research facilities used in this study. The authors also thank to Dr. David C. Apperley of the EPSRC Solid-state NMR Service, Industrial Research Laboratories, University of Durham, for his assistance in acquisition and interpretation of NMR spectra. The authors also thank to Miguel A. Ramos of the Materials Characterization and Structure Unit, Laboratory of X-ray diffraction, Zulian Technological Research Institute (Venezuela) for his assistance in acquisition of the crystallographic data.

References

1. D. Breck. *Zeolite Molecular Sieves: Structure, Chemistry and Use*. Ed. John Wiley. New York (USA). 1974. pp. 313.

2. G. Gottardi, E. Galli. *Natural Zeolites*. Ed. Springer-Verlag. Berlin (Germany). 1985. pp. 409.

3. W. Taylor. "The structure of analcime ($NaAlSi_2O_6.H_2O$)." *Zeitschrift für Kristallographie*. Vol. 74. 1930. pp. 1-19.

4. M. Calleri, G. Ferraris. "Struttura dell' analcime: $NaAlSi_2O_6.H_2O$." *Atti Ace Scienze di Torino*. Vol. 118. 1964. pp. 821-846.

5. C. Knowles, F. Rinaldi, J. Smith. "Refinement of the crystal structure of analcime." *Indian Mineralogy*. Vol. 6. 1965. pp. 127-140.

6. G. Ferraris, D. Jones, J. Yerkess. "A neutron diffraction study of the crystal structure of analcime, $NaAlSi_2O_6.H_2O$." *Zeitschrift für Kristallographie*. Vol. 135. 1972. pp. 240-252.

7. D. Coombs. "X-ray investigation on wairakite and non-cubic analcime." *Mineralogical Magazine.* Vol. 30. 1955. pp. 699-708.

8. K. Harada, T. Sudo. "A consideration on the wairakite-analcime series. Is valid a new mineral name for sodium analogue of monoclinic wairakite?" *Mineralogical Journal*. Vol. 8. 1976. pp. 247-251.

9. F. Mazzi, E. Galli. "Is each analcime different?" *American Mineralogist*. Vol. 63. 1978. pp. 448-460.

10. F. Mazzi, E. Galli, G. Gottardi. "The crystal structure of tetragonal leucite". *American Mineralogist*. Vol. 61. 1976. pp. 108-115".

11. Y. Yokomori, S. Idaka. "The crystal structure of analcime". *Microporous and Mesoporous Materials*. Vol. 21. 1998. pp. 365-370.

12. F. Pechar. "The crystal structure of natural monoclinic analcime ($NaAlSi_2O_6.H_2O$)". *Zeitschrift für Kristallographie.* Vol. 184. 1988. pp. 63-69.

13. M. Akizuki. "Origin of optical variation in analcime". *American Mineralogist*. Vol. 66. 1981. pp. 403-409.

14. M. Sandoval, J. Henao, C. Ríos, C. Williams, D. Apperley. "Synthesis and characterization of zeotype ANA framework by hydrothermal reaction of natural clinker". *Fuel.* Vol. 88. 2009. pp. 272-281.

15. A. Boultif, D. Louer. "Powder pattern indexing with the dichotomy method". *Journal of Applied Crystallography*. Vol. 37. 2004. pp. 724-731.

16. H. M. Rietveld. "A profile refinement method for nuclear and magnetic structures". *Journal of Applied Crystallography*. Vol. 2. 1969. pp. 65-71.

17. L. Lutterotti. *MAUD, Material Analysis using Diffraction*. Available from: http://www.ing.unitn.it/~luttero/maud/index.html. 18 June 2010.

18 P. Thompson, D. Cox, J. Hastings. "Rietveld refinement of Debye-Scherrer synchrotron X-ray data from Al_2O_3." *Journal of Applied Crystallography.* Vol. 20. 1987. pp. 79-83.

19 L. Finger, D. Cox, A. Jephcoat. "A correction for powder diffraction peak asymmetry due to axial divergence". *Journal of Applied Crystallography*. Vol. 27. 1994. pp. 892-900.

20. R. Young. *The Rietveld Method.* Ed. Oxford University Press. Oxford (USA). 1993. pp. 312.

21 B. Liu, D. Tang, C. Au. "Fabrication of analcime zeolite fibers by hydrothermal synthesis". *Microporous and Mesoporous Materials*. Vol. 86. 2005. pp. 106-111.

22 G. Engelhardt, D. Michel. *High Resolution Solid State NMR of Silicates and Zeolites*. Ed. Wiley & Sons. New York (USA). 1987. pp. 424.

23 R. Kirkpatrick. "MAS NMR spectroscopy of minerals and glasses". *Reviews in Mineralogy*. Vol. 18. 1988. pp. 341-403.